Biophysical Journal, Volume *118*

Supplemental Information

Liquid-Liquid Phase Separation of Histone Proteins in Cells: Role in Chromatin Organization

Anisha Shakya, Seonyoung Park, Neha Rana, and John T. King

Calculation of PONDR and ExPASy hydropathy scores. Predictor of Natural Disordered Regions (PONDR) (1) scores and Expert Protein Analysis System (ExPASy)(2) hydropathy scores were predicted using the following sequences:

H1.2 (human):

MSETVPPAPAASAAPEKPLAGKKAKKPAKAAAASKKKPAGPSVSELIVQAASSSKERGGVSLAALKKALAAAGYD
VEKNNSRIKLGIKSLVSKGTLVQTKGTGASGSFKLNKKASSVETKPGASKVATKTKATGASKKLKKATGASKKSVK
TPKKAKKPAATRKSSKNPKKPKTVKPKKVAKSPAKAKAVKPKAAKARVTKPKTAKPKKAAPKKK

H1 (calf thymus):

MTENSTSTPAAKPKRAKASKKSTDHPKYSDMIVAAIQAEKNRAGSSRQSIQKYIKSHYKVGENADSQIKLSIKRLV
TTGVLKQTKGVGASGSFRLAKSDEPKRSVAFKKTKKEVKKVATPKKAAKPKKAASKAPSKKPKATPVKKAKKKPA
ATPKKTKKPKTVKAKPVKASKPKKTKPVKPKAKSSAKRTGKKK

H2A (human):

MSGRGKQGGKARAKAKTRSSRAGLQFPVGRVHRLLRKGNYAERVGAGAPVYLAAVLEYLTAEILELAGNAARD
NKKTRIIPRHLQLAIRNDEELNKLLGKVTIAQGGVLPNIQAVLLPKKTESHHKAKGK

H2B (human):

MPEPAKSAPAPKKGSKKAVTKAQKKDGKKRKRSRKESYSIYVYKVLKQVHPDTGISSKAMGIMNSFVNDIFERIA
GEASRLAHYNKRSTITSREIQTAVRLLLPGELAKHAVSEGTKAVTKYTSAK

H3 (human):

MARTKQTARKSTGGKAPRKQLATKAARKSAPATGGVKKPHRYRPGTVALREIRRYQKSTELLIRKLPFQRLVREI
AQDFKTDLRFQSSAVMALQEACEAYLVGLFEDTNLCAIHAKRVTIMPKDIQLARRIRGERA

H4 (human):

MSGRGKGGKGLGKGGAKRHRKVLRDNIQGITKPAIRRLARRGGVKRISGLIYEETRGVLKVFLENVIRDAVTYTEH
AKRKTVTAMDVVYALKRQGRTLYGFGG

HP1α (human):

MIHHHHHHLEGKKTKRTADSSSSEDEEEYVVEKVLDRRVVKGQVEYLLKWKGFSEEHNTWEPEKNLDCPELISE
FMKKYKKMKEGENNKPREKSESNKRKSNFSNSADDIKSKKKREQSNDIARGFERGLEPEKIIGATDSCGDLMFLM
KWKDTDEADLVLAKEANVKCPQIVIAFYEERLTWHAYPEDAENKEKETAKS

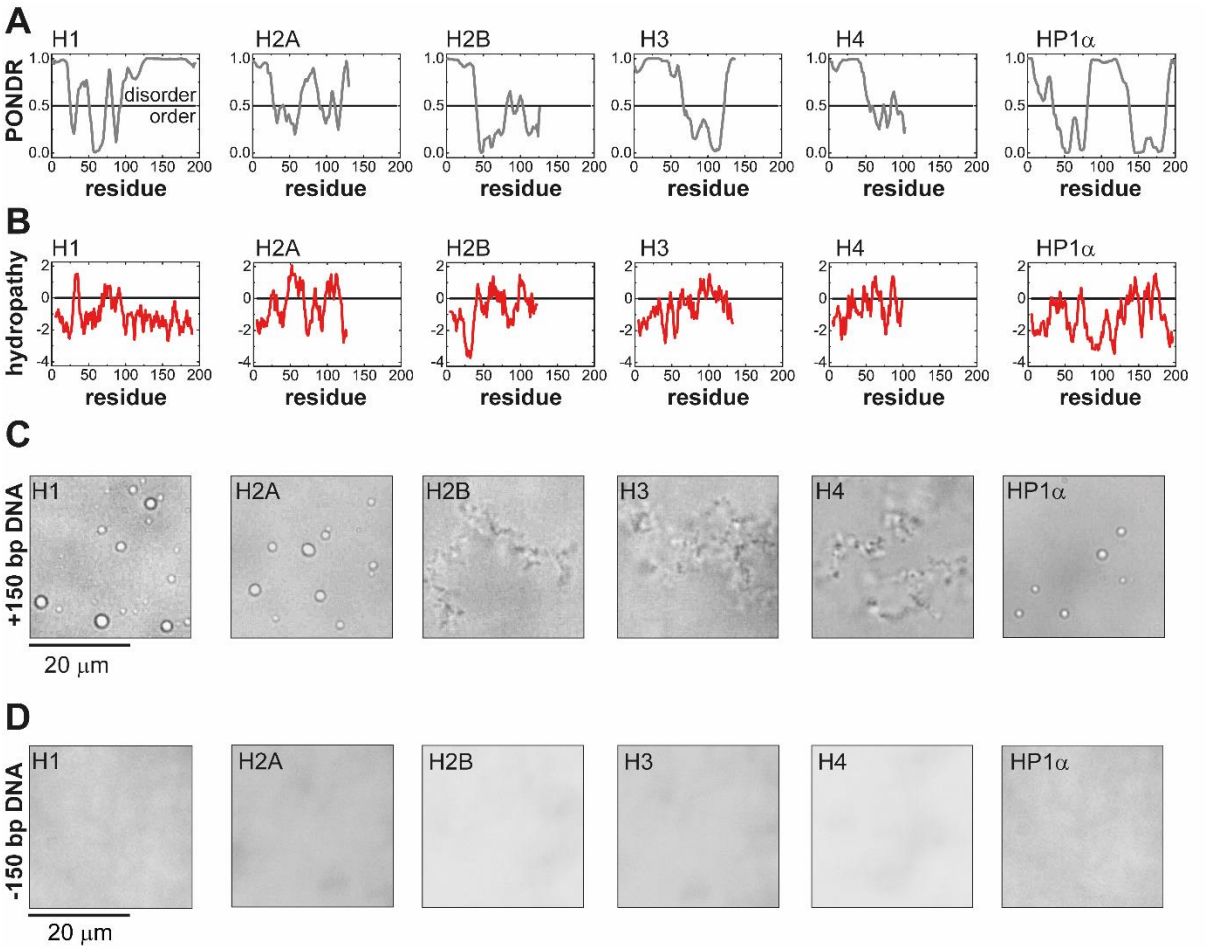

FIGURE S1. LLPS of chromatin proteins with 150 bp DNA. (**A**) PONDR scores calculated for H1, H2A, H2B, H3, H4, and HP1α (sequences used are shown above). PONDR scores above 0.5 represents significant structural disorder. (**B**) Analysis of histone and HP1 sequences showing hydropathy scores using ExPASy, where positive scores represent hydrophobic regions. (**C**) At physiological salt concentration, N/P ~1, and in presence of 150 bp DNA, H1, H2A, and HP1α undergo multi-component LLPS *in vitro*, while H2B, H3, and H4 form precipitates (also see **Fig. S7**). (**D**) Single-component LLPS is not observed at physiological salt concentration ([H1] = 0.3 μM, [H2A] = 1.0 μM, [H2B] = 1.0 μM, [H3] = 0.9 μM, [H4] = 1.0 μM, HP1α concentration = 0.1 μM).

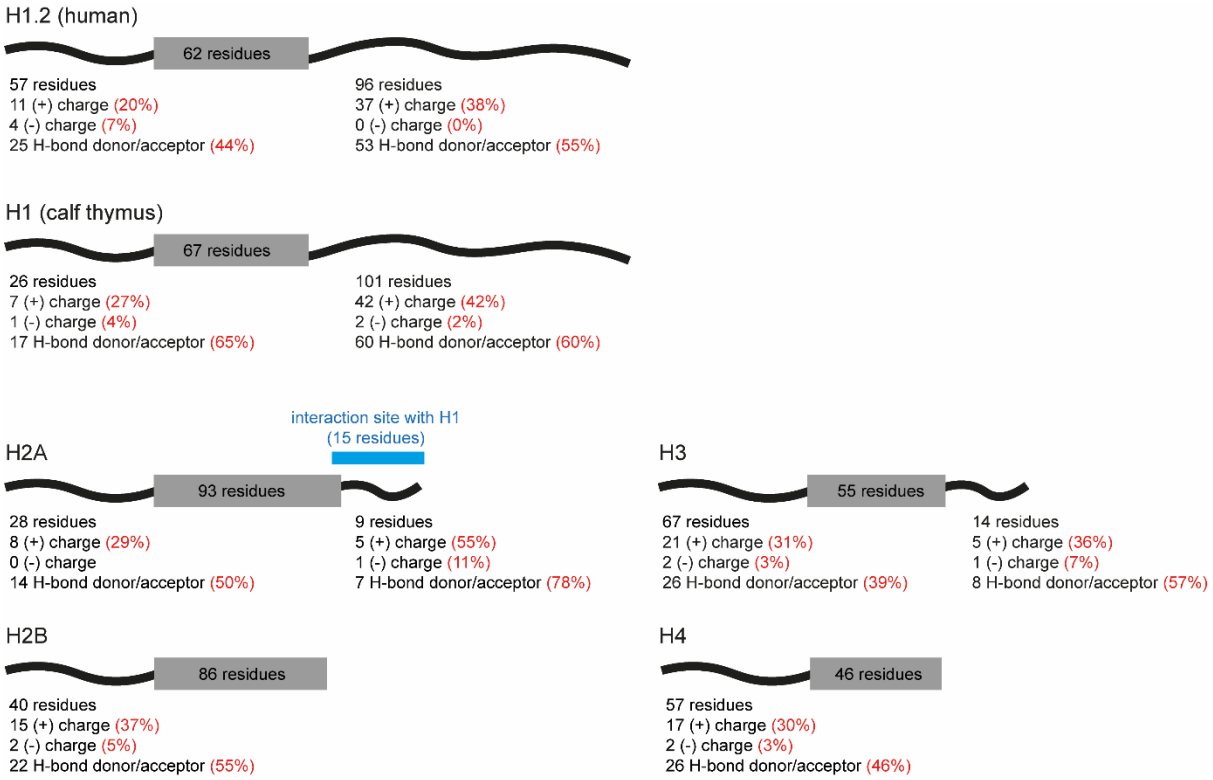

Figure S2. Visual representation of histone proteins showing length of the disordered regions of the protein as well as the number of charged residues and hydrogen bonding residues in the C-/N-terminal tails as predicted by PONDR (1).

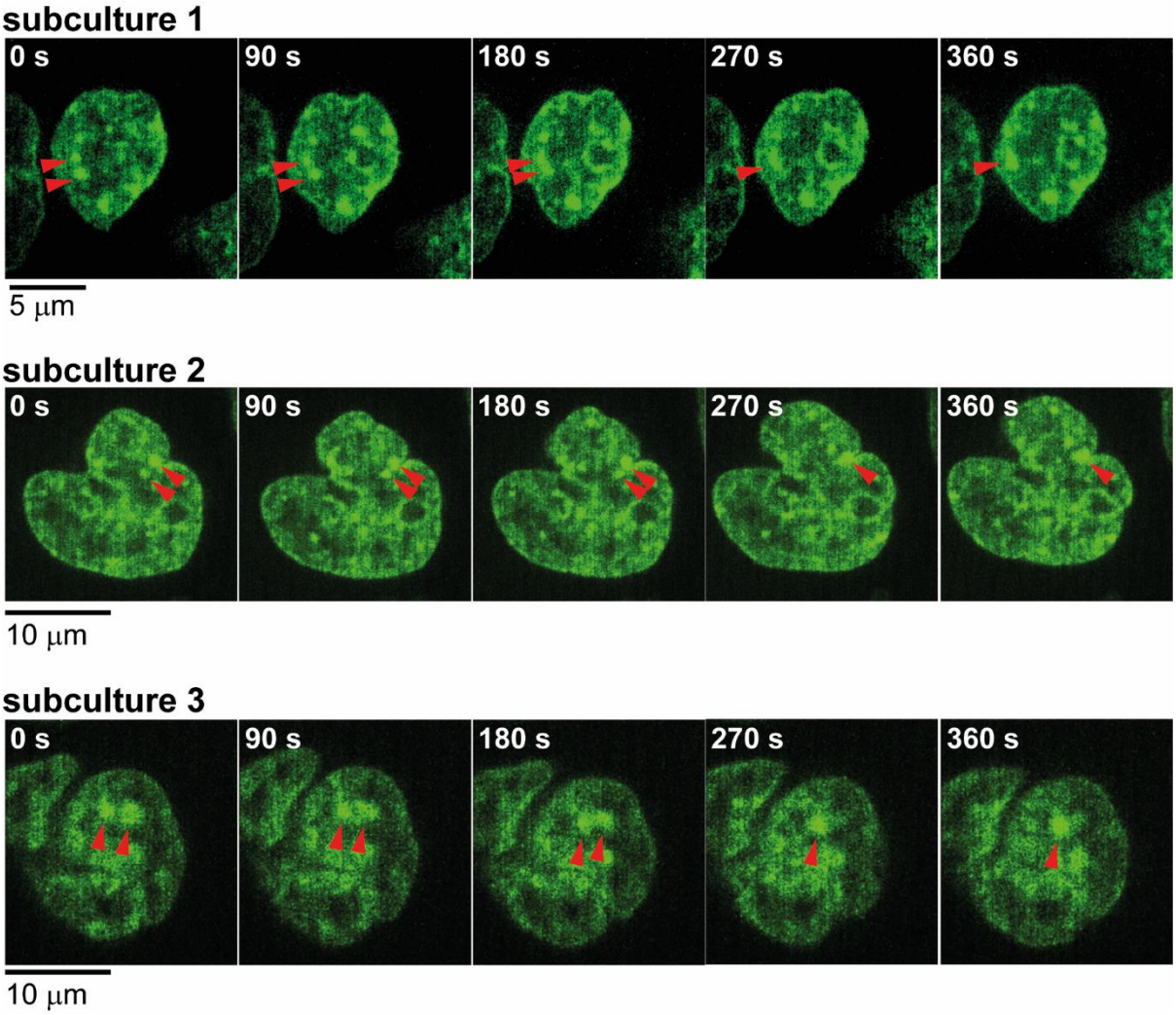

FIGURE S3. Merging dynamics of H1-DNA puncta in HeLa cell nuclei. Representative merging events in HeLa nuclei of neighboring puncta imaged in cells from three different subcultures under identical conditions.

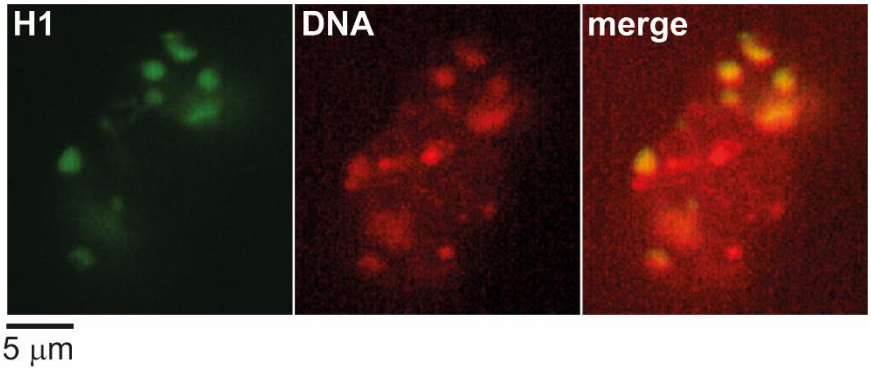

FIGURE S4. Two-color confocal microscopy images of H1-eGFP (left) and DRAQ5 stained DNA (middle) in the nucleus of a HeLa cell. The merged image (right) shows colocalization of H1 with DNA dense regions associated with heterochromatin.

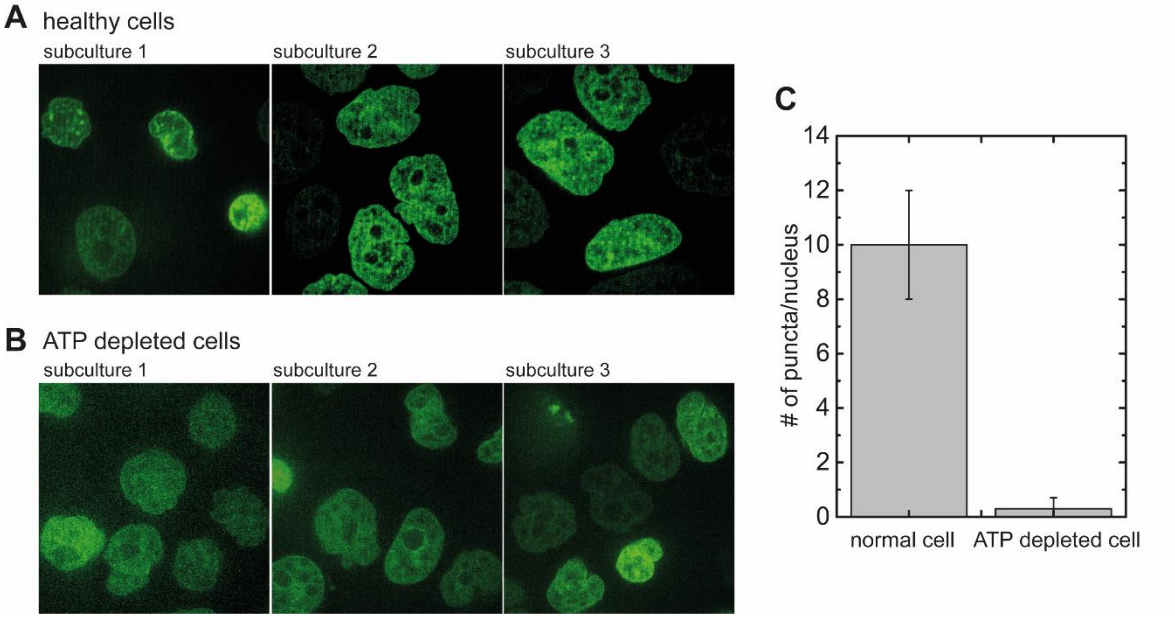

FIGURE S5. H1 puncta in (**A**) healthy cells vs (**B**) ATP depleted cells. (**C**) The number of puncta observed in healthy nuclei is ~10 puncta per nucleus, while in the nuclei of ATP depleted cells the average number of puncta observed per nuclei is less than 1. The error bars represent the standard deviation from the analysis of roughly 30 cells.

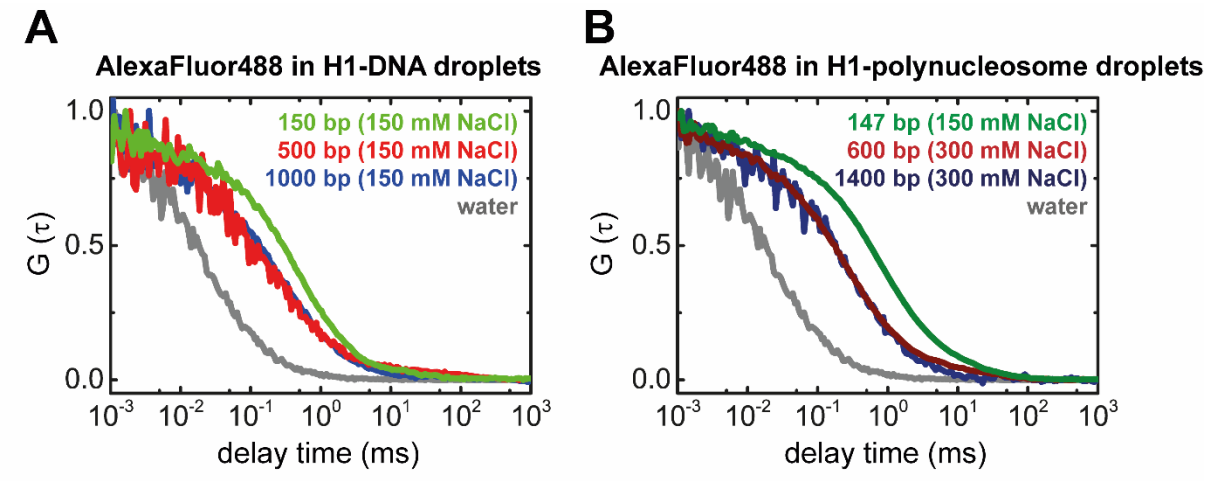

FIGURE S6. FCS of AlexaFluor488 partitioned into H1-DNA and H1-polynucleosome droplets (N/P ~1). FCS autocorrelation curves of free AlexaFluor488 in (**A**) H1-DNA and (**B**) H1-polynucleosome droplets. The ~1 ms timescale diffusion of the free dye indicates liquid-like interior. As expected for such droplets, slower diffusion of the dye is observed compared to that in DI water. Interestingly, the diffusion timescales are faster for droplets containing longer DNA/polynucleosome.

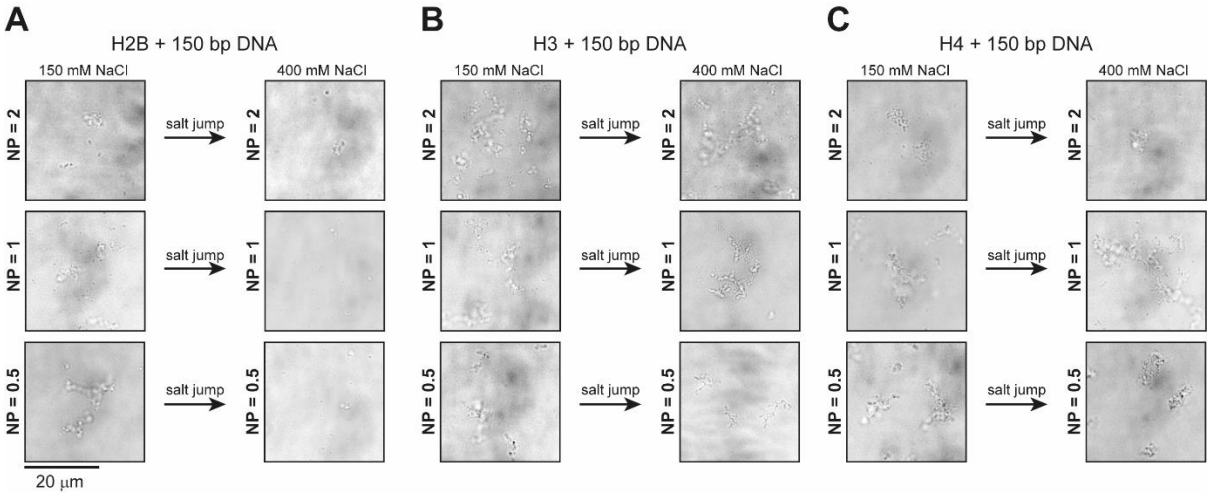

FIGURE S7. LLPS of H2B, H3, and H4, with 150 bp DNA at varying charge ratios (N/P ~0.6, N/P ~1, N/P ~1.75) at 150 mM NaCl. Pre-formed condensates were subjected to a salt jump (addition of NaCl to increase the final concentration from 150 mM to 400 mM). The aggregates of H2B/H3/H4 with DNA do not dissolve upon increased salt concentration, indicating these condensates are irreversible.

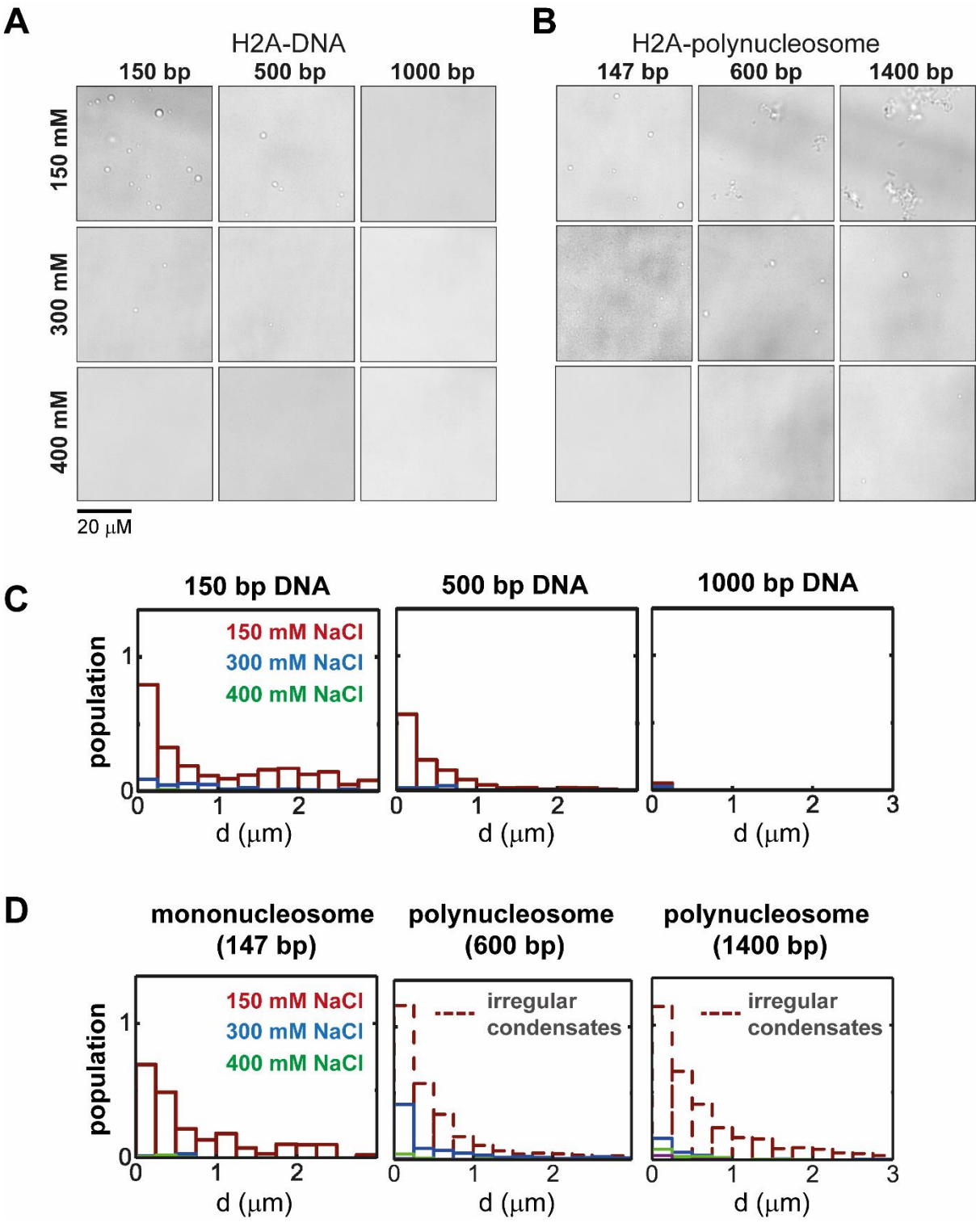

FIGURE S8. Phase diagram and droplet size analysis for H2A-DNA and H2A-polynucleosome. Bright-field microscopy images of (**A**) H2A-DNA and (**B**) H2A-polynucleosome mixtures with varying salt concentrations and DNA length (N/P ~1). The images were acquired ~2 h after mixing. (**C-D**) Droplet population statistics vs droplet size (diameter, *d*) for each experimental condition obtained from analysis of 10 images per experiment.

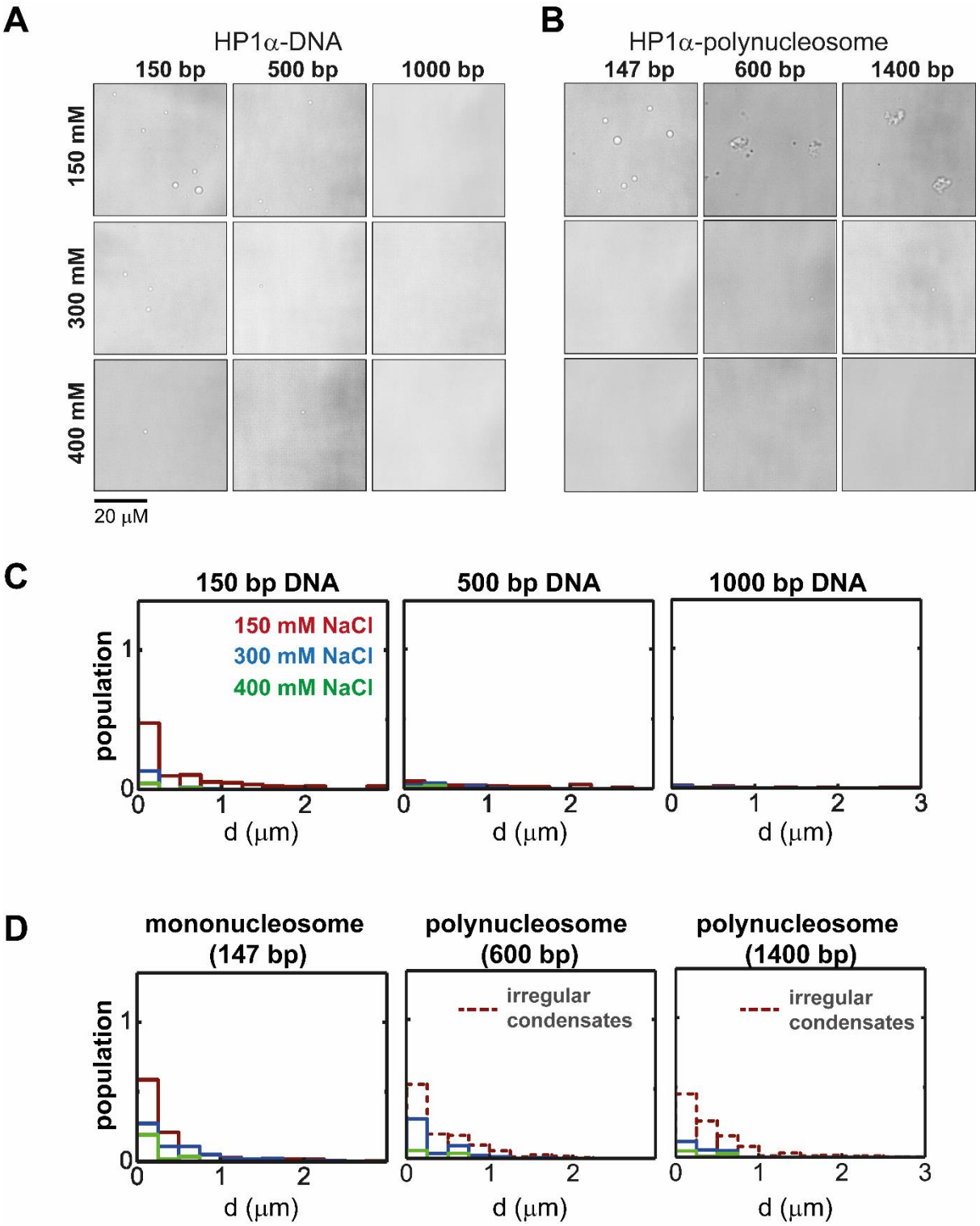

FIGURE S9. Phase diagram and droplet size analysis for HP1α-DNA and HP1α-polynucleosome. Bright-field microscopy images of (**A**) HP1α-DNA and (**B**) HP1α-polynucleosome mixtures with varying salt concentrations and DNA length (N/P ~0.9). The images were acquired ~2 h after mixing. (**C-D**) Droplet population statistics vs droplet size (diameter, *d*) for each experimental condition obtained from analysis of 10 images per experiment.

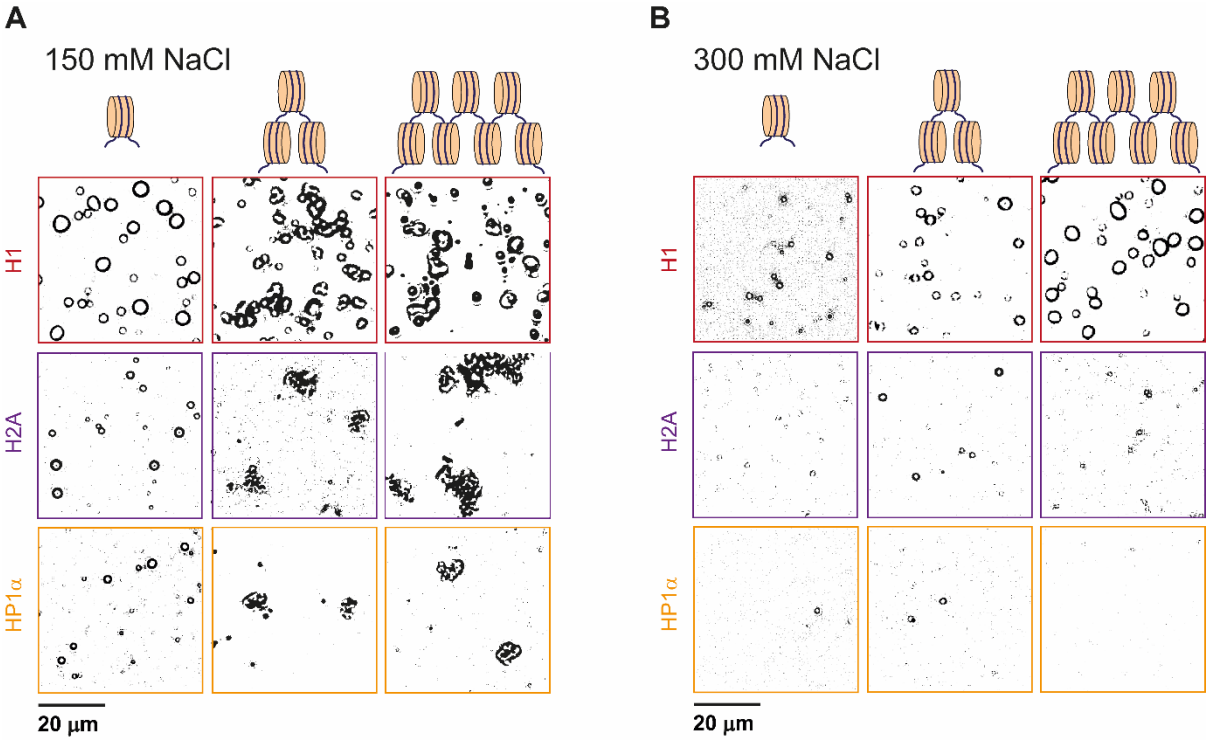

FIGURE S10. Representative bright-field microscopy images (contrasted with ImageJ) of H1/H2A/HP1α-polynucleosome droplets (N/P ~1) as a function of polynucleosome length at (**A**) 150 mM NaCl and (**B**) 300 mM NaCl.

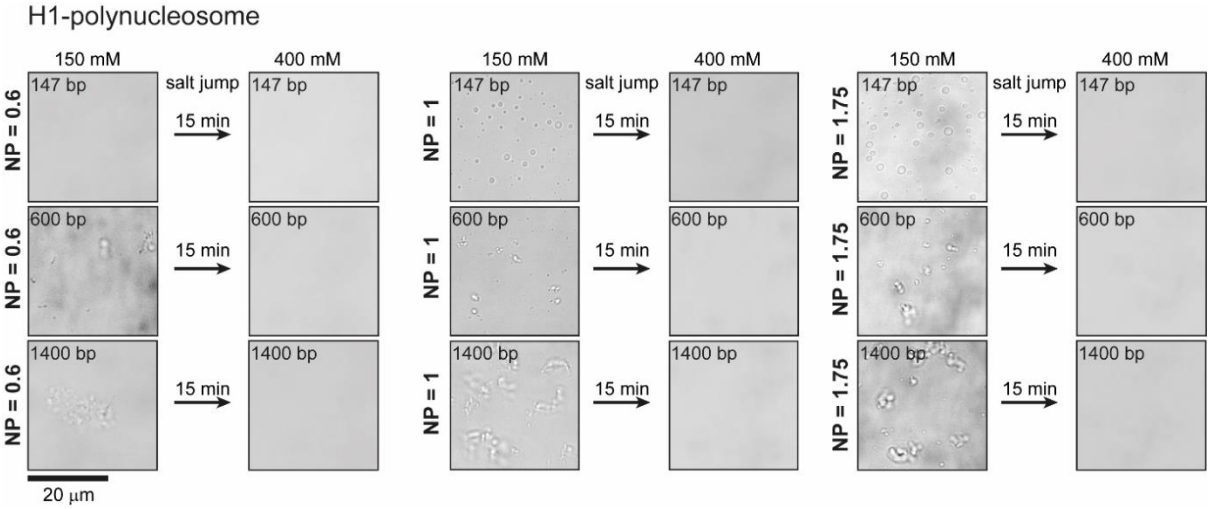

FIGURE S11. H1-polynucleosome LLPS at varying charge ratio (N/P ~0.6, N/P ~1, N/P ~1.75) at 150 mM NaCl. Pre-formed condensates were subjected to a salt jump (addition of NaCl to increase the final concentration from 150 mM to 400 mM). Both H1-mononucleosome and H1-polynucleosome condensates dissolve upon increased salt concentration, indicating reversibility of the condensates.

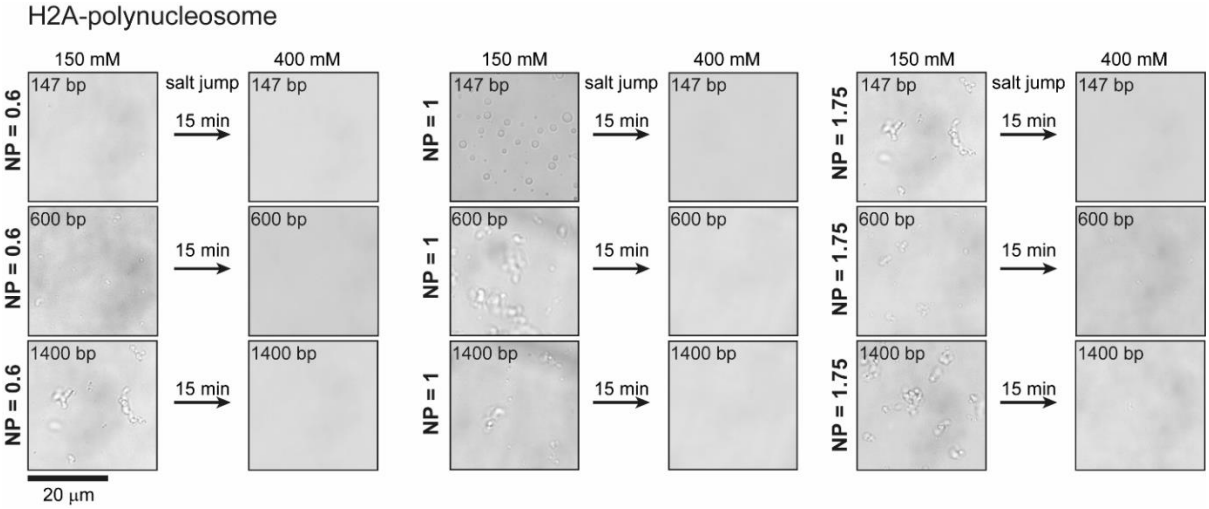

FIGURE S12. H2A-polynucleosome LLPS at varying charge ratio (N/P ~0.6, N/P ~1, N/P ~1.75) at 150 mM NaCl. Pre-formed condensates were subjected to a salt jump (addition of NaCl to increase the final concentration from 150 mM to 400 mM). Both H2A-mononucleosome and H2A-polynucleosome condensates dissolve upon increased salt concentration, indicating reversibility of the condensates.

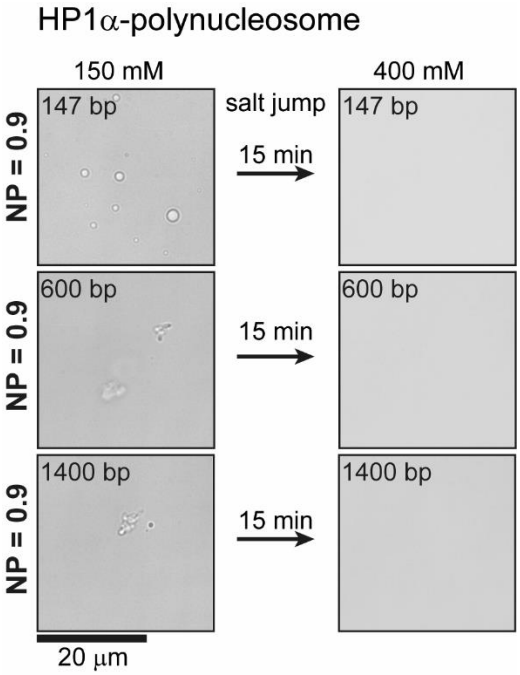

FIGURE S13. HP1α-polynucleosome LLPS at 150 mM NaCl (N/P ~ 0.9). Pre-formed condensates were subjected to a salt jump (addition of NaCl to increase the final concentration from 150 mM to 400 mM). Both HP1α-mononucleosome and HP1α-polynucleosome condensates dissolve upon increased salt concentration, indicating reversibility of the condensates.

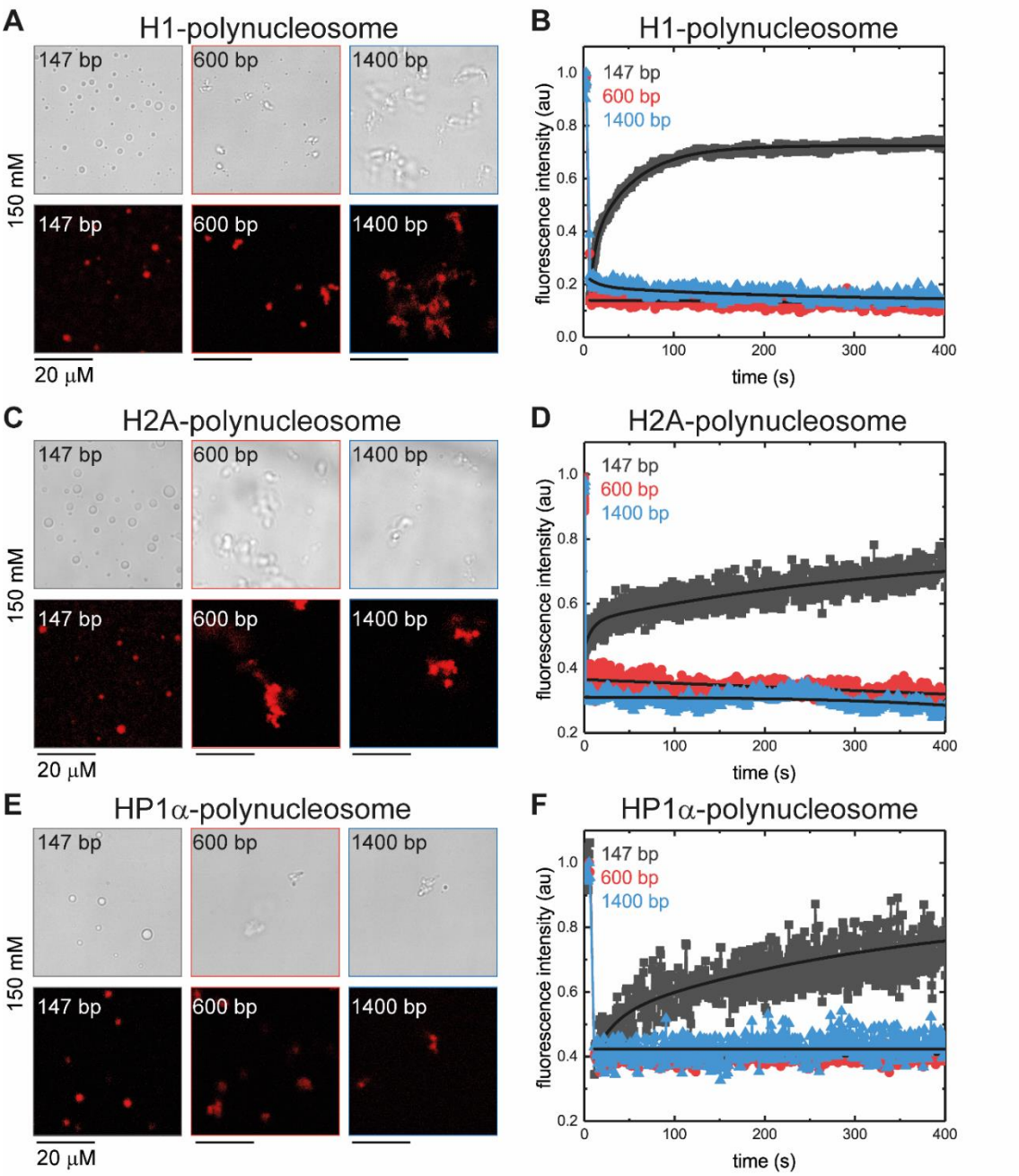

FIGURE S14. Fluorescence recovery after photobleaching (FRAP) experiments on AlexaFluor488 labeled (**A-B**) H1, (**C-D**) H2A, (**E-F**) HP1α partitioned into protein-nucleosome condensates formed at 150 mM NaCl and N/P ~1. For H1, H2A, and HP1α, the protein component is mobile in condensates formed with mononucleosomes, which form spherical droplets at 150 mM NaCl, indicated by recovery of the fluorescence signal after photobleaching. However, in condensates formed from polynucleosomes, which form irregular condensates at 150 mM NaCl, no fluorescence recovery is observed following photobleaching, indicating that the protein component is dynamically arrested. Each FRAP curve is the average of 3 experiments.

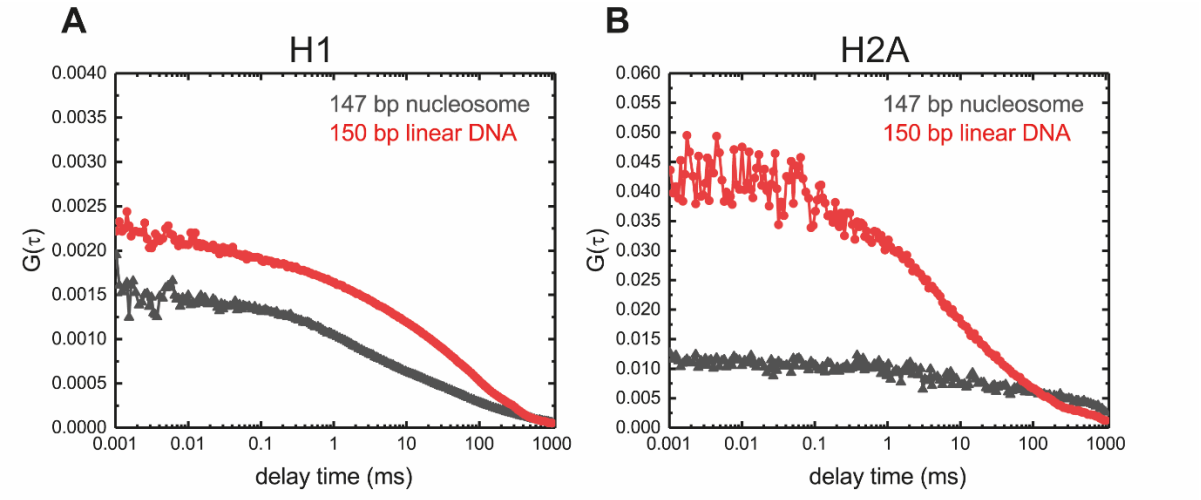

FIGURE S15. Fluorescence correlation spectroscopy (FCS) of AlexaFluor488 labeled (**A**) H1 and (**B**) H2A in droplets formed with mononucleosome (grey) and 150 bp linear DNA (red) at 150 mM NaCl and N/P ~1. H1 partitions more strongly into the droplets compared to H2A, as evidenced by the significantly smaller G_0 value. Additionally, H1 and H2A partition more strongly into nucleosome-based droplets compared to linear DNA-based droplets, as evidenced by the smaller G_0 value. H1 concentrations within condensates were estimated to be 2.4 mM and 1.4 mM in nucleosome and DNA based droplets, respectively. H2A concentrations within condensates were estimated to be 0.8 mM and 0.4 mM in nucleosome and DNA based droplets, respectively.

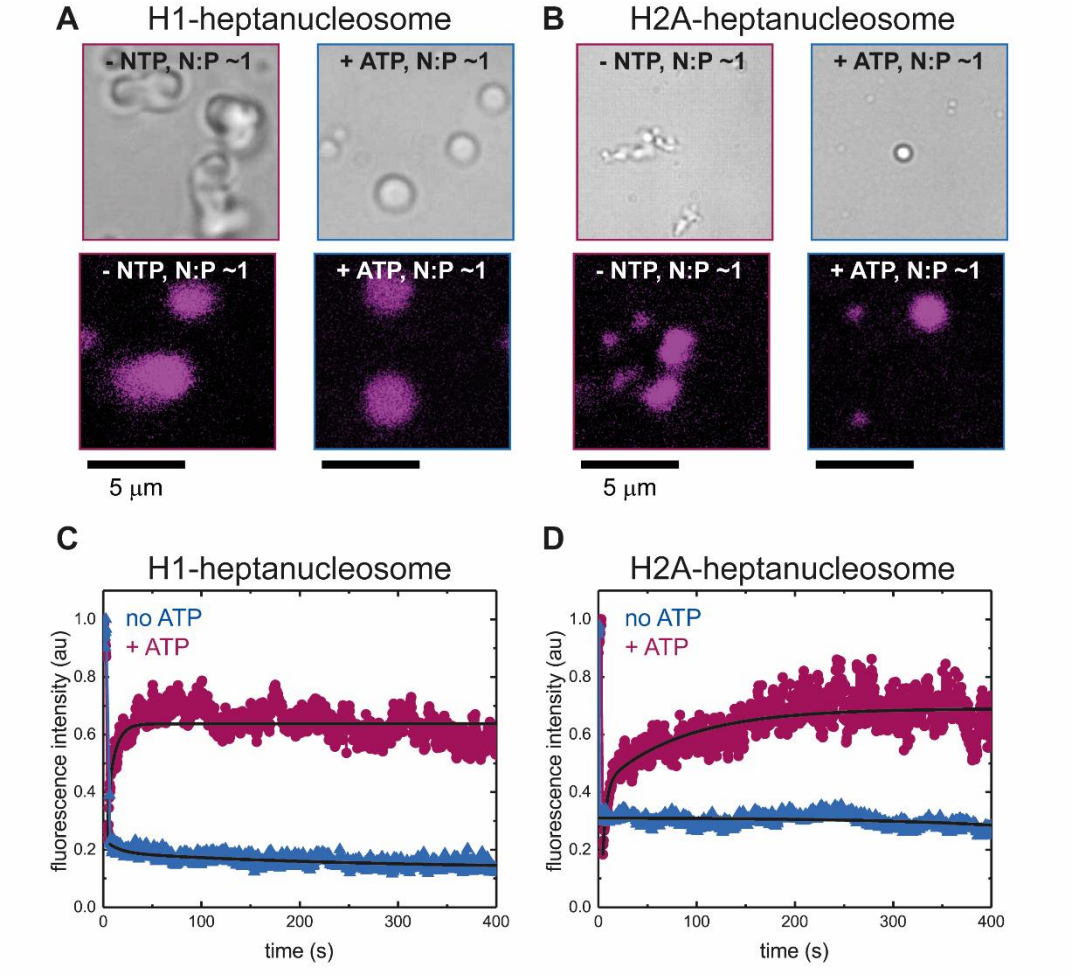

FIGURE S16. Fluorescence recovery after photobleaching (FRAP) experiments on AlexaFluor488 labeled (**A**) H1 (**B**) H2A partitioned into the protein-heptanucleosome condensates formed at 150 mM NaCl and N/P ~1, in presence and absence of ATP. In presence of ATP, the protein component is mobile (both H1 and H2A), indicating a liquid-like environment of the condensates. Each FRAP curve is the average of 3 experiments.

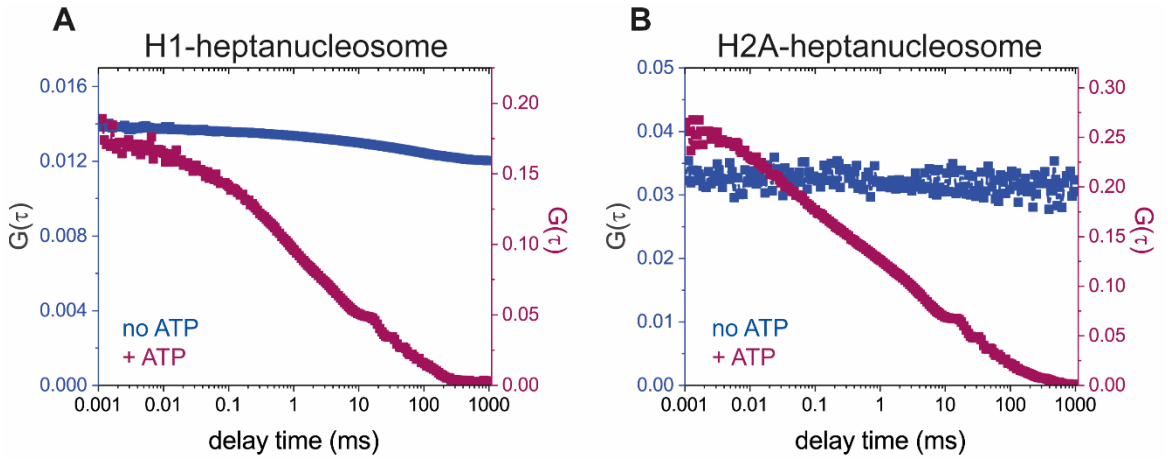

Figure S17. Fluorescence correlation spectroscopy (FCS) experiments on AlexaFluor488 labeled (**A**) H1 and (**B**) H2A partitioned into protein-polynucleosome condensates formed at 150 mM NaCl and N/P ~1, in presence and absence of ATP. In presence of ATP, the protein component is mobile (both H1 and H2A), indicating a liquid-like environment of the condensate.

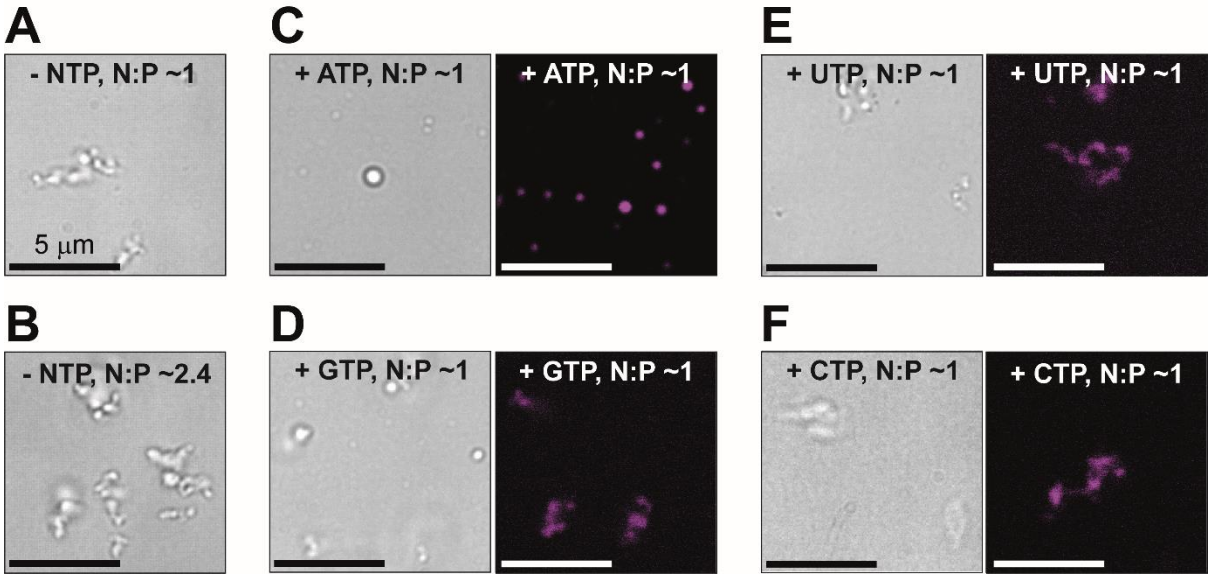

FIGURE S18. H2A-polynucleosomes (1400 bp) form irregular condensates in absence of ATP at physiological salt concentration at (**A**) N/P ~1 and (**B**) N/P ~2.4 (reduced polynucleosome concentration). (**C-F**) Representative bright-field and confocal images of fluorescently labeled NTPs ((**C**) ATP; (**D**) GTP; (**E**) UTP; (**F**) CTP; all at a concentration of 1.5 μm) show the presence of ATP promotes H1-polynucleosomes (1400 bp) LLPS into spherical, liquid-like droplets at physiological salt concentration (N/P ~1). However, GTP, UTP, and CTP show coarse condensates at the same concentration.

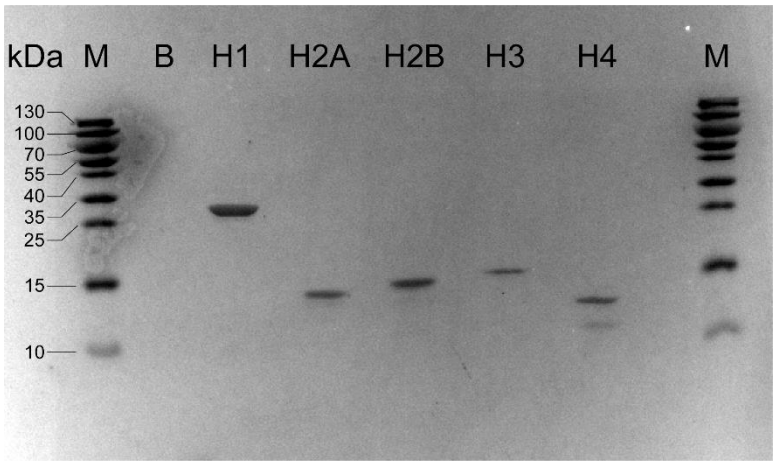

FIGURE S19. SDS-PAGE of histone proteins.

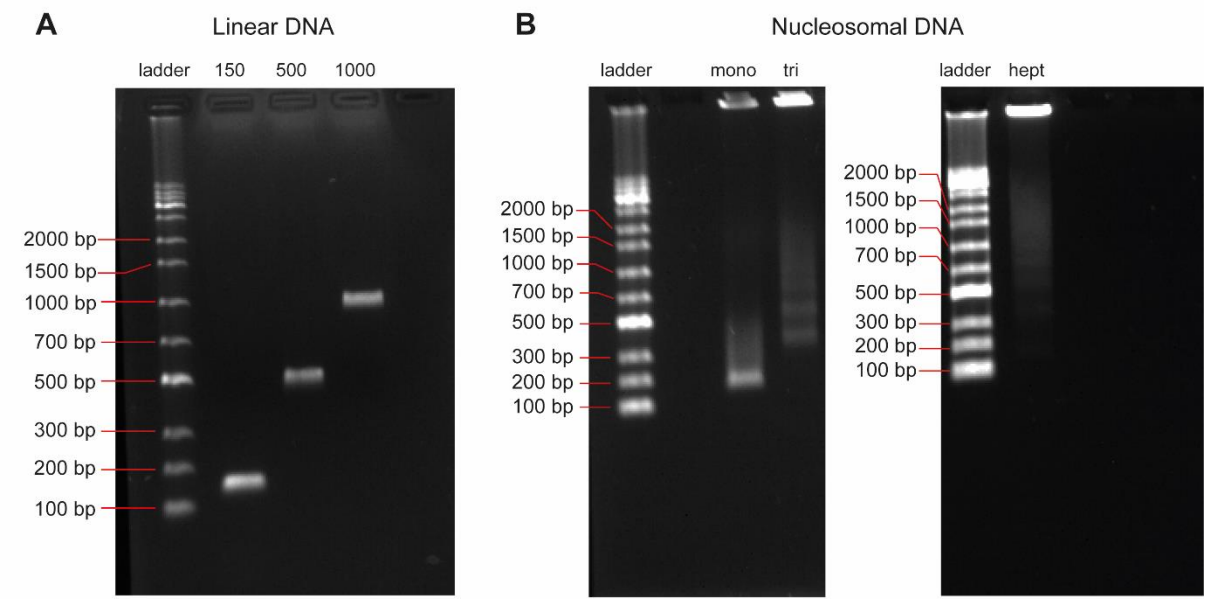

FIGURE S20. Agarose gel electrophoresis of (**A**) free DNA and (**B**) nucleosomes.

REFERENCES

1. Romero, P., Z. Obradovic, X. H. Li, E. C. Garner, C. J. Brown, and A. K. Dunker. 2001. Sequence complexity of disordered protein. *Proteins-Structure Function and Genetics* 1:38-48.
2. Gasteiger, E., A. Gattiker, C. Hoogland, I. Ivanyi, R. D. Appel, and A. Bairoch. 2003. ExPASy: the proteomics server for in-depth protein knowledge and analysis. *Nucleic Acids Res.* 13:3784-3788.